# Boundary-induced wavelength selection in a one-dimensional pattern-forming system

Samuel S. Mao and John R. de Bruyn
*Department of Physics, Memorial University of Newfoundland, St. John's, Newfoundland, Canada A1B 3X7*

Zahir A. Daya and Stephen W. Morris
*Department of Physics and Erindale College, University of Toronto, 60 St. George Street, Toronto, Ontario, Canada M5S 1A7*

(Received 27 March 1995; revised manuscript received 26 March 1996)

We have measured the stability boundary for steady electroconvection in thin, freely suspended smectic liquid crystal films. As the voltage across the film, or the film length, is varied, convective vortices are created or destroyed at the ends of the film to keep the pattern wave number within a stable range. The measured stability boundary lies substantially inside the Eckhaus boundary for this system. Our results are consistent with a mechanism for boundary-induced wavelength selection proposed by Cross *et al.* [Phys. Rev. Lett. **45**, 898 (1980)]. [S1063-651X(96)50308-9]

PACS number(s): 47.20.−k, 47.54.+r

The formation and dynamics of patterns in nonequilibrium nonlinear systems has been the subject of much recent study [1]. The general behavior of fully three-dimensional (3D) systems can be quite complicated, so there is substantial interest in systems that develop simpler, one-dimensional (1D) patterns which can be subjected to detailed experimental and theoretical study. Many such systems have been studied, including fluid dynamical systems such as Rayleigh-Bénard convection (RBC) and Taylor-vortex flow (TVF) [1,2]. Although any real fluid system is 3D, if the spatial structure of the flow *pattern* is characterized by a 1D wave vector $k$ we refer to the pattern as one-dimensional. An important issue in the study of patterns is that of wave number selection [1]. Typically, beyond the onset of the pattern state, the spatially uniform base state will be unstable to perturbations within a band of wave numbers. This reflects the fact that the nonlinear equations and boundary conditions describing the system do not have a unique solution, but rather admit a multiplicity of solutions. The range of wave numbers over which the pattern is stable is limited to a narrower band by various secondary instabilities. The wave number actually observed will depend on the system's history and geometry, and will be within the stable band selected by the instabilities of the system. Some of these secondary instabilities are intrinsically 2 or 3D [1], and can be partly suppressed by geometrically confining the system in the direction perpendicular to $k$. Some wave number selection mechanisms, however, are purely 1D. Slow spatial variation of the control parameter through its value at the pattern onset will select a unique wave number [3,4]. The Eckhaus instability [5] is a long-wavelength phase instability which results in the creation or loss of pattern units. It has been studied in detail, for example, in TVF [4], for which the amplitude of the pattern remains large near the ends of the experimental cell. If the amplitude goes to zero at the ends, as it does in RBC, rolls can be created or destroyed there, resulting in a change of wave number [6]. This mechanism, which has been studied theoretically by Cross *et al.* (CDHS) [6], results in a stability range significantly narrower than the Eckhaus-stable range close to onset. Numerical simulations of RBC have shown roll creation and loss at end walls and provide qualitative support for the theory of CDHS [7,8]. In an RBC experiment, Martinet *et al.* [9] observed wall-mediated wave number adjustments and a restricted band of stable wave numbers which, near onset, qualitatively agreed with the predictions of CDHS. Three-dimensional effects were important in their experimental system, however [1,9], and as yet there has been no unambiguous experimental observation of boundary-induced wave number selection.

In this Rapid Communication we report measurements of the stability boundary of patterns of electrically driven convective vortices in very thin, freely suspended films of smectic-*A* liquid crystal [10,11]. Smectics-A have a layered structure [12] which makes it possible to make uniformly thick centimeter-size films, a small number of smectic layers thick (one layer = 3.16 nm). Flow between the layers is very difficult, and a film behaves as a 2D isotropic fluid [11]. Since the films are very thin, instabilities involving a bending or reorientation of the vortex axes are impossible, and we expect only 1D processes to be involved in wave number selection.

Our experimental apparatus is similar to that used previously [10,11]. The long sides of the film were supported by two 23-$\mu$m-diameter tungsten wire electrodes. The ends of the film were supported by thin plastic wipers which rested on the wires. The separation of the electrodes $d$ was adjustable; for the work reported here $0.66<d<2$ mm. One of the end wipers could be driven with a motorized micrometer, allowing variation of the film length $L$ in the range $0<L<30$ mm. Films were made by bringing the two wipers together, placing a small amount of liquid crystal [13] on the place where they joined, and then slowly drawing them apart. A voltage $V$ is applied between the two electrodes, and a steady, 1D array of counter-rotating convection vortices appears at a well-defined critical voltage $V_c$ [10]. This pattern persists up to a certain voltage, beyond which the flow becomes unsteady. The films can maintain their uniform thickness in the presence of strong convection, or, if $L$ is

 

varied, by exchanging material with a small wetting layer on the electrodes or wipers. The film holder was temperature controlled to $\pm 0.1$ °C over a given run. All runs were performed at temperatures in the range $25 \pm 1$ °C, well below the smectic-*A*–nematic transition at 33 °C. The films were viewed through a microscope with a color charge-coupled-device video camera. Smoke particles were allowed to settle on the film, and were made visible by a beam of white light directed onto the film from below. Flow was visualized by following the particles as they were advected by flow in the film.

The onset voltage $V_c$, and thus the dimensionless control parameter [11] $\epsilon = (V/V_c)^2 - 1$ depend on the film thickness $s$, which we measured in two ways. $s$ is on the order of a wavelength of visible light, so the films show bright interference colors when viewed in reflected white light. The color of the film can be calculated in terms of the CIE chromaticity diagram [14], and with practice, $s$ can be determined by eye for films up to about 100 layers thick. We also determined $s$ from reflectivity measurements [15]. For $s < 10$ layers, the change in reflectivity due to a one-layer change in $s$ is large compared to the experimental uncertainties and the thickness determination is exact. For films between 10 and 100 layers thick, these two techniques used together allow determination of $s$ with an accuracy of $\pm 1$ layer.

We measured the stability boundary of the steady convective state using two techniques. In the first, a stable pattern was prepared by increasing the applied voltage above the onset of convection. Patterns with wave numbers $k$ close to $k_c$, the wave number at onset [10], were obtained by increasing $V$ slowly through the pattern onset, while a sudden jump from below to substantially above $V_c$ resulted in a pattern with $k$ different from $k_c$. Roughly speaking, jumping to values of $\epsilon$ in the range $1 \lesssim \epsilon \lesssim 4$ gave $k < k_c$, while jumping to $\epsilon \gtrsim 4$ resulted in a pattern with $k > k_c$. The voltage was then changed in small steps and the flow pattern monitored. The pattern required of order 50 vortex turnover times, or about 1 min, to equilibrate after a change in $V$. Typically, varying the voltage eventually led to a wave number adjustment through the creation or loss of a vortex, which always occurred at the ends of the film, not in its interior.

In the second type of measurement, a stable pattern was prepared as above. The film length was then changed at constant thickness by slowly ($\approx 20$ $\mu$m/s) moving the motorized wiper. As shown in Fig. 1, as $L$ is increased (solid circles), the wavelength $\lambda$ increases, to accommodate the change in length at fixed number of vortices. Eventually $\lambda$ reaches a value above which the pattern is unstable. At this point one or more new vortices form at the end of the film, and the mean wavelength of the pattern decreases back to a stable value. When the film length is decreased (open circles) the opposite process occurs, with a vortex disappearing at the end of the film when $\lambda$ decreases below the stable range. As above, the creation and destruction of vortices occurred at the ends of the film [16], and, as shown in Fig. 1, was always hysteretic [17].

Figure 2 shows the stability range of the steady vortex pattern measured with these two techniques. Data from 36 runs, using films with thickness between 2 and 45 layers, and with aspect ratios $\Gamma = L/d$ in the range $3 < \Gamma < 15$, were combined to produce the points plotted as solid symbols, which represent the maximum and minimum values of $\epsilon$ at which a given wave number state was observed at fixed $L$. No systematic variation in the position of the boundary with either $s$ or $\Gamma$ was detected. The open symbols in Fig. 2 show the

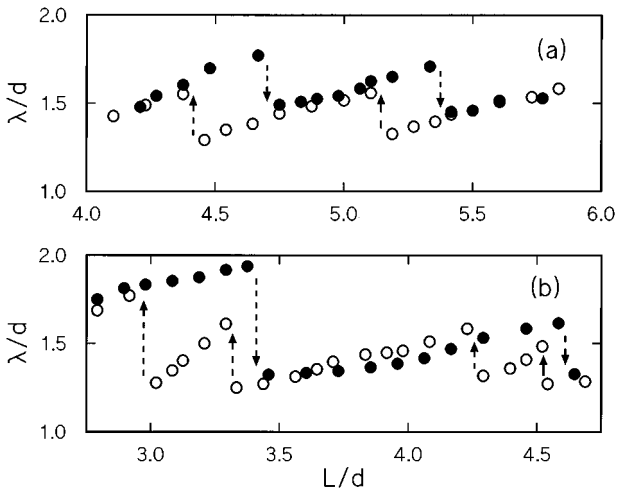


FIG. 1. The pattern wavelength as function of film length, both normalized by the film width $d$, as the film length was varied. The wavelength plotted is the mean over the pattern, excluding the vortices at the ends of the film. The solid and open circles were obtained by increasing and decreasing $L$, respectively. Arrows indicate wavelength changes caused by the creation or loss of vortices. (a) $s = 50$ layers, $\epsilon = 1.0$; single vortices are gained or lost at the arrows. (b) $s = 25$ layers, $\epsilon = 3.0$; two vortices are gained simultaneously at the downward arrows; they are lost one at a time at the upward arrows.

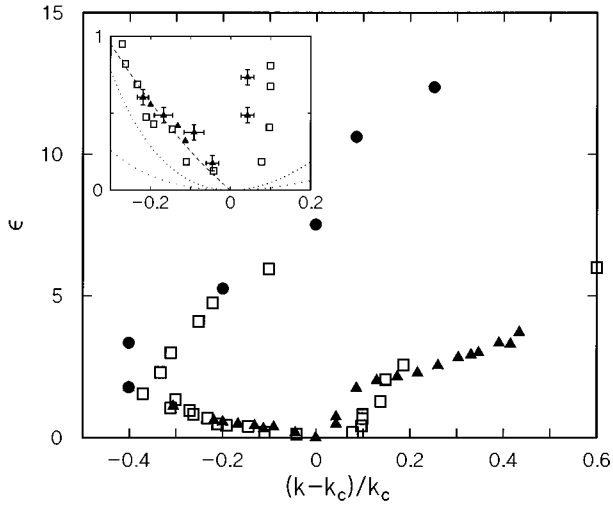


FIG. 2. The stable wave number range for steady electroconvection. The solid symbols were determined by increasing (circles) or decreasing (triangles) the applied voltage at constant film geometry. The open squares were determined by varying the film length at constant voltage. The inset shows the data for $\epsilon < 1$. The lower and upper dotted lines are the marginal stability curve and the Eckhaus stability boundary, respectively, calculated from a linear stability analysis for this system [19]. The dashed line is a fit of the data for $\epsilon < 1$, $k < k_c$ to the form $\epsilon = a(k-k_c)/k_c + b[(k-k_c)/k_c]^2$ which gives $a = -2.2 \pm 0.5$ and $b = 3.2 \pm 2.3$.

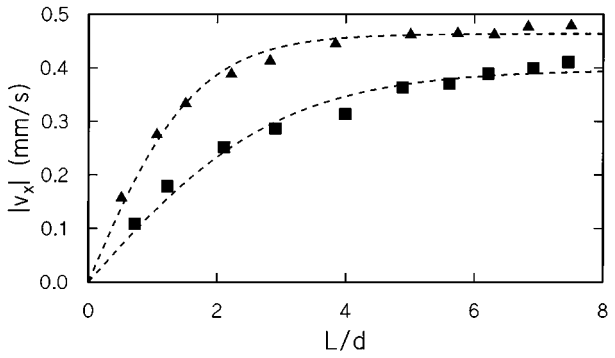


FIG. 3. The maximum of the $x$ component of the flow velocity within each vortex as a function of position along a film, for $\epsilon=0.06$ (squares) and $\epsilon=0.13$ (triangles). $v_x$ was measured a distance $d/5$ from the two electrodes. The dashed curves are fits to a tanh function, the form predicted by the Ginzburg-Landau equation [2]. The amplitude of the flow pattern becomes small near the ends of the cell.

stability boundary determined by varying $L$ at fixed $\epsilon$, as in Fig. 1, and indicate the range of $k$ observed at different values of $\epsilon$. Data from 20 runs with films having $s$ between 3 and 65 layers and $2<\Gamma<15$ are shown. Again there were no systematic variations in the boundary with either $s$ or $\Gamma$. The inset to Fig. 2 shows the same data for $\epsilon<1$. The stability boundaries measured with both techniques are consistent in their general shape over the whole range of measurements, and for $k-k_c<0$ and $\epsilon\lesssim 2$, the two boundaries agree very well. The quantitative differences in other parts of the diagram may be due to variations in the conditions at the ends of the films, as the small amount of liquid crystal remaining on the wipers after the film has been drawn is different in every run.

We have also performed a theoretical linear stability analysis for this system [19]. The two dotted curves in the inset to Fig. 2 are the marginal stability curve $\epsilon_m(k)$ calculated from that analysis, and the curve $\epsilon_E(k)=3\epsilon_m(k)$, which is an approximation to the Eckhuas stability boundary valid at small $\epsilon$. Our measured stability boundary lies well inside the Eckhaus boundary at small $\epsilon$.

The flow velocity can be measured by tracking the motion of the visualization particles on the film. Figure 3 shows the maximum magnitude of the flow velocity in the $x$ direction (parallel to the electrodes) in each vortex, as a function of $x$ for $\epsilon=0.06$ and 0.13. This quantity, which is essentially the amplitude of the pattern, decreases near the ends of the film. From these and similar data, we have determined the characteristic length scale $\xi_0$ of the pattern [20,21], from which the Eckhaus boundary at small $\epsilon$ can be calculated [1,2]. The result is consistent with the Eckhaus boundary shown in Fig. 2.

CDHS have studied the effects of end walls on wave number selection in RBC [6]. The amplitude of the convection pattern is weaker near a wall than in the bulk. This implies that it is easier to create or destroy convection rolls there. CDHS calculated the range of stable wave numbers for this situation and found it to be linear, i.e., $\epsilon_B\propto|(k-k_c)/k_c|$, in contrast to the quadratic boundary, $\epsilon_E\propto|(k-k_c)/k_c|^2$, found for the Eckhaus instability [1,5]. Thus at small enough $\epsilon$, the effect of end walls results in a narrower stable band than would the Eckhaus instability. The slope of the lower-$k$ boundary of the stable region must be negative, but that of the higher-$k$ boundary can have either sign, depending, for RBC, on the fluid properties and on the exact nature of the boundary conditions at the end walls [6].

The theory of CDHS was derived in the context of RBC but can be applied to any 1D pattern-forming system in which the pattern can be described by the appropriate amplitude equation, and for which the pattern amplitude is suppressed at the end walls. The onset of convection in our system develops via a supercritical bifurcation, and so, near onset, it can be described by a Landau equation. Recently we have analyzed our electroconvection patterns at and above onset in terms of a Ginzburg-Landau equation, and found good agreement with the predicted behavior [20]. The boundary conditions in our system are that the convective pattern amplitude goes to zero at the rigid end supports of the film, as shown in Fig. 3, and analogous to the situation for RBC. Thus we fully expect the theory of CDHS to be applicable to our system. We note, however, that the end conditions in our experiments also involve the electric field that drives the flow, which will be modified by the presence of the wipers, and by the excess liquid crystal which remains on the wipers. In the context of the theory of CDHS, this might affect the quantitative results, such as the slopes of the two branches of the stability boundary, but not their linear form.

Since our films are extremely thin and the convection pattern is thus extremely one-dimensional, the only mechanisms which can play a role in wave number selection are the Eckhaus instability and the boundary-induced wavelength selection mechanism of CDHS. The data in Fig. 2 show that for $\epsilon\lesssim 1$, the measured stability range is significantly narrower than the Eckhaus-stable range, particularly for $k>k_c$. The dashed curve plotted in the inset to Fig. 2 is a fit of the function $\epsilon=a(k-k_c)/k_c+b[(k-k_c)/k_c]^2$ to both sets of data for $\epsilon<1$, $k<k_c$, with $a$ and $b$ parameters. This fit describes the data in this range well, while, in contrast, a fit with no linear term does not. Finally, in our experiments vortices form or vanish at the ends of the system, not in the interior. These results are all consistent with the predictions of CDHS, but not with those expected from the Eckhaus instability.

In summary, we have studied wave number selection in electrically driven convection in freely suspended smectic films. Because of the extreme two-dimensionality of the films, effects due to 3D flow, or to bending of the convection roll axis, do not exist in this system. Wave number adjustments occur via the creation or loss of vortices at the ends of the film. The band of stable wave numbers broadens linearly, and is significantly narrower than the Eckhaus stability boundary, for small $\epsilon$. These results are consistent with those expected if the wavelength selection is induced by end effects related to the fact that the pattern amplitude becomes small near the end wall, as predicted theoretically by CDHS [6], but are inconsistent with the Eckhaus mechanism.

We are grateful to M. Cross for a helpful discussion, and to G. Ahlers for a critical reading of this paper. This research was supported by the Natural Sciences and Engineering Research Council of Canada.

[1] M. C. Cross and P. C. Hohenberg, Rev. Mod. Phys. **65**, 851 (1993).
[2] G. Ahlers, in *Lectures in the Sciences of Complexity*, edited by D. Stein (Addison, Reading, MA, 1989), p. 175.
[3] L. Kramer, E. Ben-Jacob, H. Brand, and M. C. Cross, Phys. Rev. Lett. **49**, 1891 (1982).
[4] M. A. Dominguez-Lerma, D. S. Cannell, and G. Ahlers, Phys. Rev. A **34**, 4956 (1986).
[5] W. Eckaus, *Studies in Nonlinear Stability Theory* (Springer, New York, 1965).
[6] M. C. Cross, P. G. Daniels, P. C. Hohenberg, and E. D. Siggia, Phys. Rev. Lett. **45**, 898 (1980); J. Fluid Mech. **127**, 155 (1983).
[7] J. C. Mitais, P. Haldenwang, and G. Labrosse, in *Proceedings of the VIII International Heat Transfer Conference*, edited by C. L. Tien, V. P. Carey, and J. K. Ferell (Harper and Row, New York, 1986), p. 1545.
[8] W. Arter, A. Bernoff, and A. C. Newell, Phys. Fluids **30**, 3840 (1987).
[9] B. Martinet, P. Haldenwang, G. Labrosse, J. C. Payan, and R. Payan, in *Cellular Structures in Instabilities*, edited by J. E. Wesfreid and S. Zaleski (Springer-Verlag, Berlin, 1984), p. 33
[10] S. W. Morris, J. R. de Bruyn, and A. D. May, Phys. Rev. Lett. **65**, 2378 (1990); J. Stat. Phys. **64**, 1025 (1991).
[11] S. W. Morris, J. R. de Bruyn, and A. D. May, Phys. Rev. A **44**, 8146 (1991).
[12] P. G. de Gennes and J. Prost, *The Physics of Liquid Crystals*, 2nd ed. (Clarendon, Oxford, 1993).
[13] The material used was 4,4′-*n*-octylcyanobiphenyl (8CB) doped with $7.5 \pm 0.2$ mM/1 tetracyanoquinodimethan (TCNQ) to control the nature of the ionic species in the liquid crystal.
[14] E. B. Sirota, P. S. Pershan, L. B. Sorensen, and J. Collett, Phys. Rev. A **36**, 2890 (1987).
[15] C. Rosenblatt and N. Amer, Appl. Phys. Lett. **36**, 432 (1980).
[16] At higher voltages, close to the onset of the unsteady state, we occasionally observed vortices created or destroyed in the interior of the film. Away from that transition, the wavelength adjustments always took place at the ends.
[17] Techniques analogous to ours were used by Dominguez-Lerma *et al.* [4] to measure the stability boundary of Taylor-Couette flow; they observe the creation or loss of Taylor vortex pairs in the interior of the system, and their measured stability boundary was in quantitative agreement with the calculated Eckhaus stability boundary [18].
[18] H. Riecke and H. G. Paap, Phys. Rev. A **33**, 547 (1986).
[19] Z. Daya, S. W. Morris, and J. R. de Bruyn (unpublished).
[20] S. S. Mao, J. R. de Bruyn, and S. W. Morris, Physica A (to be published).
[21] J. Wesfreid, Y. Pomeau, M. Dubois, C. Normand, and P. Bergé, J. Phys. (Paris) **39**, 725 (1978).